



A theoretical and experimental benchmark study of core-excited states in nitrogen

Myhre, Rolf H.; Wolf, Thomas J. A.; Cheng, Lan; Nandi, Saikat; Coriani, Sonia; Gühr, Markus; Koch, Henrik

Published in:
Journal of Chemical Physics

Link to article, DOI:
[10.1063/1.5011148](https://doi.org/10.1063/1.5011148)

Publication date:
2018

Document Version
Peer reviewed version

[Link back to DTU Orbit](#)

Citation (APA):
Myhre, R. H., Wolf, T. J. A., Cheng, L., Nandi, S., Coriani, S., Gühr, M., & Koch, H. (2018). A theoretical and experimental benchmark study of core-excited states in nitrogen. *Journal of Chemical Physics*, 148(6), [064106]. <https://doi.org/10.1063/1.5011148>

General rights

Copyright and moral rights for the publications made accessible in the public portal are retained by the authors and/or other copyright owners and it is a condition of accessing publications that users recognise and abide by the legal requirements associated with these rights.

- Users may download and print one copy of any publication from the public portal for the purpose of private study or research.
- You may not further distribute the material or use it for any profit-making activity or commercial gain
- You may freely distribute the URL identifying the publication in the public portal

If you believe that this document breaches copyright please contact us providing details, and we will remove access to the work immediately and investigate your claim.

A theoretical and experimental benchmark study of core-excited states in nitrogen

Rolf H. Myhre,^{1,2,3} Thomas J. A. Wolf,⁴ Lan Cheng,⁵ Saikat Nandi,^{6,7} Sonia Coriani,^{8,9}
Markus Gühr,^{4,10} and Henrik Koch^{2,3,a)}

¹⁾*Hylleraas Centre for Quantum Molecular Sciences, Department of Chemistry,
University of Oslo, 0315 Oslo, Norway*

²⁾*Department of Chemistry, Norwegian University of Science and Technology,
7491 Trondheim, Norway*

³⁾*Department of Chemistry and the PULSE Institute, Stanford University, Stanford,
California 94305, USA*

⁴⁾*Stanford PULSE Institute, SLAC National Accelerator Laboratory, Menlo Park,
CA 94025, US*

⁵⁾*Department of Chemistry, The Johns Hopkins University, Baltimore,
Maryland 21218, USA*

⁶⁾*Synchrotron SOLEIL, L'Orme des Merisiers, Saint-Aubin, BP 48,
91192 Gif-sur-Yvette Cedex, France*

⁷⁾*Department of Physics, Lund University, P. O. Box 118, SE-221 00 Lund,
Sweden.*

⁸⁾*Department of Chemistry, Technical University of Denmark, DK-2800,
Kongens Lyngby, Denmark*

⁹⁾*Aarhus Institute of Advanced Studies, Aarhus University, DK-8000, Århus C,
Denmark*

¹⁰⁾*Department of Physics and Astronomy, University of Potsdam, 14476 Potsdam,
Germany*

(Dated: 8 January 2018)

The high resolution near edge X-ray absorption fine structure spectrum of nitrogen displays the vibrational structure of the core-excited states. This makes nitrogen well suited for assessing the accuracy of different electronic structure methods for core excitations. We report high resolution experimental measurements performed at the SOLEIL synchrotron facility. These are compared with theoretical spectra calculated using coupled cluster theory and algebraic diagrammatic construction theory. The coupled cluster singles and doubles with perturbative triples model known as CC3 is shown to accurately reproduce the experimental excitation energies as well as the spacing of the vibrational transitions. The computational results are also shown to be systematically improved within the coupled cluster hierarchy, with the coupled cluster singles, doubles, triples and quadruples method faithfully reproducing the experimental vibrational structure.

Keywords: Coupled Cluster, Nitrogen, NEXAFS, Response theory

^{a)}Corresponding author. Electronic mail:henrik.koch@ntnu.no, henrik.koch@sns.it

I. INTRODUCTION

X-ray absorption spectroscopy (XAS) is a well established technique that provides a unique ability to study local properties of molecules. The most intense X-ray sources are large synchrotrons, but more recently, X-ray free electron lasers (XFEL) have made time dependent experiments feasible. Inauguration and construction of new FEL X-ray sources such as the European XFEL, SwissFEL, PALFEL SNAP and LCLS II demonstrate that the field is in rapid development. Furthermore, recent developments in high harmonics generation have made ultrafast X-ray experiments feasible in a tabletop setting. In order to fully utilize the power provided by such experiments, accurate theoretical methods are required to interpret the results¹⁻¹².

Simulating high photon energy processes such as near edge X-ray absorption fine structure (NEXAFS) spectra involves a number of challenges not encountered in low energy processes such as UV/Vis spectroscopy. Exciting an electron from a core orbital involves a significant reduction in the screening of the core, leading to large relaxation effects. The most important ones are contraction of the valence electron density and repulsion due to the electron transferred from the core. Accounting for these effects theoretically is challenging. For example, results from density functional theory often have to be shifted 10 eV or more to agree with experimental results,^{13,14} and most methods require shifts of more than 1 eV.¹⁵⁻¹⁷ More recently, the extended second order algebraic diagrammatic construction (ADC(2)-x) method has produced results within a few tenths of an eV from experimental values. However, the accuracy appears to rely on the cancellation of the remaining errors in the treatment of basis set and electron correlation¹⁸.

Another challenge when computing core-excited states is that they are embedded in a continuum of Rydberg states. Most electronic structure methods involve solving an eigenvalue problem in order to determine excited electronic states. Usually, some version of the Davidson algorithm¹⁹ is used for this. It solves the eigenproblem iteratively starting with extremal eigenvalues, normally the lowest one. This is not a good approach for core excitations because there will be many excited states with lower energy. Several methods have been proposed to overcome this problem. In the Δ SCF method,²⁰ the energy of the excited state is calculated by restricting the occupation in the core orbitals and taking the energy difference from the ground state. Another approach is to solve for the eigenvalues using Krylov-

space techniques including the asymmetric Lanczos or the Arnoldi algorithm^{17,21-23}. With these algorithms, the eigenvalues are typically solved for the whole spectrum simultaneously. However, they typically become numerically unstable if the vectors are not orthogonalized at each iteration. This requires the storage of a large number of vectors on disk and limits the size of systems where such methods can be applied without further manipulations.

Arguably the most successful approach to determine the core-excited states is the core-valence separation (CVS) approach.²⁴ The energy differences between the core and valence orbitals are typically several hundred eVs. Consequently, their overlap integrals become very small and the coupling between them can be neglected. The CVS approach is utilized in ADC²⁵⁻²⁷ and has also been implemented in the coupled cluster (CC) framework²⁸. Comparing CVS and full space calculations using the Lanczos approach, discrepancies are typically less than 50 meV in our experience.

Recently, we reported a new implementation of coupled cluster singles and doubles with perturbative triples (CC3).^{29,30} This implementation has now been expanded with the CVS approximation. In this paper, we will use an experimental spectrum of nitrogen to assess the accuracy of CC3 for core-excited states. We note that N₂ has been used to assess the accuracy of ADC before²⁶. The vibrational structure in the spectrum makes it possible to evaluate the shape of the potential energy surface (PES) and to determine the effect of vibrations on the excitation energy. Comparing different levels of CC theory reveals that the vibrational structure is highly sensitive to the shape and position of the PES. Because N₂ only has 14 electrons, it is possible to use very large basis sets and minimize the basis set error which can be several eVs for core excitations. In addition, calculations with CC singles, doubles and triples (CCSDT) and CC singles, doubles, triples and quadruples (CCSDTQ) have also been carried out for this small molecule to study the higher-order correlation effects described by the full inclusion of the triple and quadruple excitations, using the recent efficient implementation of the CCSDT and CCSDTQ methods^{31,32}. The scalar-relativistic corrections have been obtained using the spin-free exact two-component theory in its one-electron variant^{33,34}.

In section II, we will briefly summarize CC theory and the CVS approximation and describe our computational and experimental approach. In section III, we present our results and section IV contains our concluding remarks and future perspective.

II. COMPUTATIONAL AND EXPERIMENTAL DETAILS

In CC theory, the wave function is written as the exponential of the cluster operator, T , acting on the Hartree-Fock (HF) reference state.

$$|\text{CC}\rangle = \exp(T) |\text{HF}\rangle \quad (1)$$

$$T = \sum_{\mu} t_{\mu} \tau_{\mu} \quad (2)$$

The excitation operators, τ_{μ} , take the reference state to an excited state in the Fock space, $|\mu\rangle = \tau_{\mu} |\text{HF}\rangle$, and t_{μ} is the corresponding amplitude. In exact theory, the CC formulation is equivalent to full configuration interaction (FCI) up to a normalisation factor, but in practice the cluster operator is truncated at some excitation level and the amplitude equations solved with projection.

$$\begin{aligned} E &= \langle \text{HF} | \exp(-T) H \exp(T) | \text{HF} \rangle \\ \Omega_{\mu} &= \langle \mu | \exp(-T) H \exp(T) | \text{HF} \rangle = 0 \end{aligned} \quad (3)$$

When calculating time dependent properties such as excitation energies and transition moments, the standard methods are CC linear response^{35,36} (CCLR) and equation of motion CC (EOM-CC).³⁷ Both methods require the eigenvalues of the nonsymmetric Jacobian matrix \mathbf{A} , whose elements are defined as the derivatives of Ω .

$$A_{\mu\nu} = \frac{\partial \Omega_{\mu}}{\partial t_{\nu}} = \langle \mu | \exp(-T) [H, \tau_{\nu}] \exp(T) | \text{HF} \rangle \quad (4)$$

The eigenvalues of the Jacobian correspond to the vertical excitation energies of the system and it is sufficient to only solve from one side if other properties are not required. If transition moments and other excited state properties are desired, it is necessary to solve the eigenvalue problem from both the left and the right hand side. As mentioned in the introduction, the eigenproblems are typically solved using an iterative procedure like the Davidson method.¹⁹

In order to obtain core-excited states, the CVS approximation has been used. In this approximation, elements coupling the core and valence-excited states are projected out. One way to implement this is by setting the elements of the eigenvectors/trial vectors not involving the core orbitals to zero at each iteration of the Davidson algorithm²⁸. Alternatively, one can explicitly restrict the excitation space to excitations originating from a core orbital

when computing the excitation energies. In this way, the core-excited and valence-excited states are completely decoupled and the algorithm will converge to the lowest core-excited states.

CCSD and CC3 calculations were performed using the Dalton program package³⁸ while CCSDT and CCDTQ calculations were done with the CFOUR program package^{31,32,39}. Scalar-relativistic effects have been taken into account in the CCSDT and CCSDTQ calculations using the spin-free exact two-component theory in its one-electron variant (SFX2C-1e)^{33,34,40}. ADC(2)-x calculations were carried out with the Q-Chem program package⁴¹. A new implementation in Dalton were used for the CC3 calculations³⁰.

Vibrational analysis was performed using the VIBROT⁴² program by Sundholm. The PESs were generated using splines between 21 single point energies for ADC(2)-x and CCSD and 22 points for the other methods. The extra point was included to describe a $^1\Sigma_u^+$ avoided crossing, but had no effect on the calculated ground state vibrational energies. Right and left moments were vibrationally averaged separately and multiplied together afterwards. Rotational levels are not resolved in the experimental spectrum and all calculated rotational transitions are for $J = 0$.

The CVS approximation^{27,28} was used for all the calculations presented here. Due to the very close energies of $1\sigma_u$ and $1\sigma_g$ orbitals, excitations from both had to be included. All CC calculations were performed using the d-aug-cc-pCVQZ^{43,44} basis set, except that the CCSDTQ calculations were performed using the cc-pCVTZ basis. The ADC(2)-x calculations were performed with aug-cc-pCVQZ because d-aug-cc-pCVQZ was not available in QChem. The difference in CC3 ground state energy between aug-cc-pCVQZ and d-aug-cc-pCVQZ is 0.26 mE_h and the difference in the first excitation energy is 0.1 meV. The quadruples contribution from cc-pCVTZ were also added to CCSDT/d-aug-cc-pCVQZ in a model labeled CCSDT+ Δ Q. CCSD oscillator strengths were calculated using CCLR in the length gauge and theoretical spectra are plotted with an empirical Lorentzian line broadening of 0.06 eV half width at half maximum. Vibrational and total energies are given in the supplemental material⁴⁵.

The experimental spectrum was recorded at room temperature at the PLÉIADES soft X-ray beamline, SOLEIL synchrotron, France⁴⁶ by measuring the total X-ray induced electron yield. The resolution was set around 50 meV and we obtained slightly better resolved vibrational features than documented in the standard paper by Chen et al.⁴⁷. We calibrated

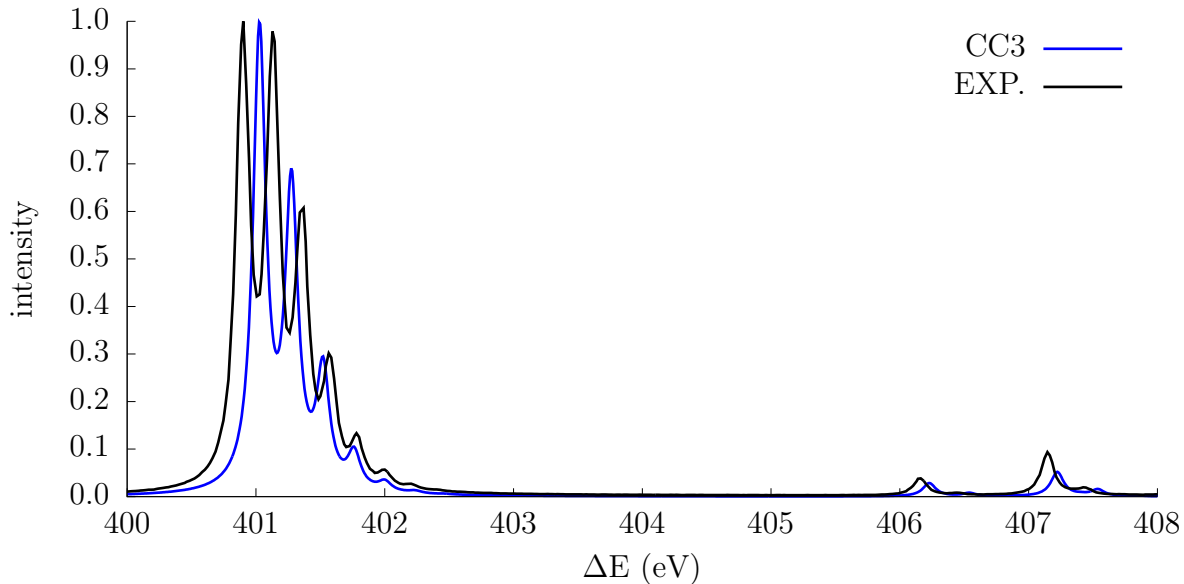


FIG. 1: Comparison of CC3 and experiment for the four lowest excited states. The intensity of the first peak is normalized to 1 and empirical line broadening added to the theoretical spectrum.

the offset of the spectrum using the electron energy loss result from Ref. 48. Details of the experimental setup at PLÉIADES are available from Ref. 49.

III. RESULTS

In Figure 1, we compare the first experimental peaks with the theoretical spectrum. Energies of the excited states were computed using CC3 while the transition moments were determined at the CCSD level.

Six electronic states give rise to the peaks in the spectrum. The peaks between 400 and 403 eV are by far the most intense and correspond to excitations from $1\sigma_u$ to two sets of equivalent π_g^* orbitals. Double excitations from [SONIA: 'involving' instead of 'from'?] the $1\sigma_g$ and π_u valence orbitals relax the electron density and must be included in the active CVS space. If the $1\sigma_g$ is not included in the active space, the calculated excitation energy is increased by more than 8 eV at CC3 level. With CCSD, the doubles component of the excitation vector contributes 11.5% and is completely dominated by excitations from $1\sigma_g$. A comparable calculation for the core excitation of oxygen in CO had the same weight of the doubles, but only involved the single [SONIA: Do you mean 'the $1s_O$?'] core orbital.

At about 406.2 eV, the first Rydberg state appears. This is a $^1\Sigma_u^+$ state where an electron

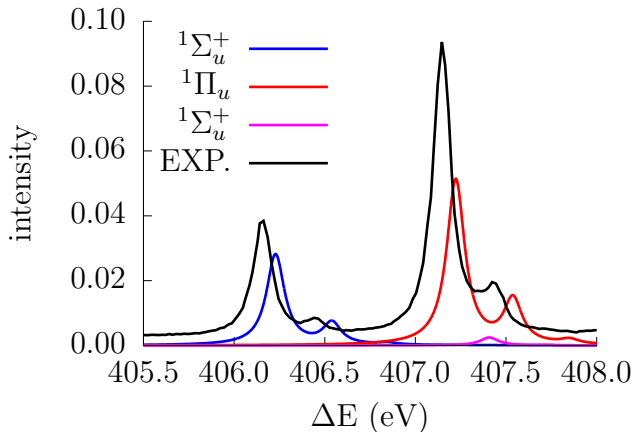


FIG. 2: Comparison of the simulated and experimental Rydberg spectra.

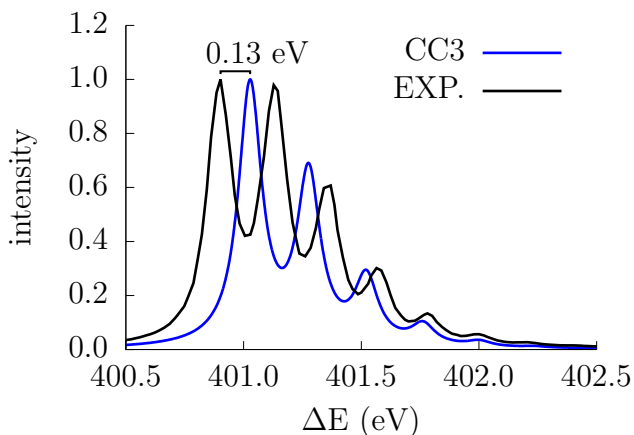


FIG. 3: Comparison of the first peak in the experimental and CC3 with d-aug-cc-pCVQZ spectra.

is excited from the core σ_u to σ_g^* . The last peak is a combination of two $^1\Pi_u$ states with the excitation of $1\sigma_g$ to the two equivalent π_u^* orbitals, and a $^1\Sigma_u^+$ state with the excitation from $1\sigma_g$ to a σ_u^* orbital. Vibrational structure is observed for all these states except the last $^1\Sigma_u^+$ state, which is too weak and convoluted with the much stronger $^1\Pi_u$ states, see Figure 2. These assignments are consistent with those of Chen *et al.*⁴⁷

Figure 3 shows the vibrational structure of the lowest core-excited state in closer detail, with the calculated positions and relative intensities of the peaks presented in Table I. **Only transitions detectable in the spectrum are presented.** The absolute error in the position of the $0 \rightarrow 0$ transition is 0.13 eV in CC3 while the distance between the vibrational levels is 0.02 eV too high. Figure 4 compares the spectra obtained with ADC(2)-x and CCSD to the experiment. For ADC(2)-x, the position of the first transition is 1.65 eV too low

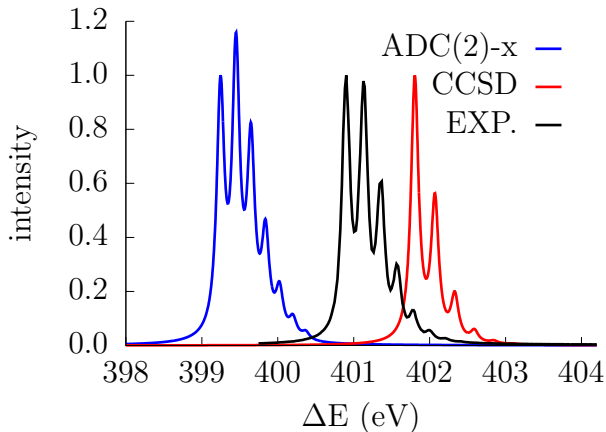


FIG. 4: Comparison of ADC(2)-x, CCSD with d-aug-cc-pCVQZ and experiment. CCSD is too high and ADC is too low.

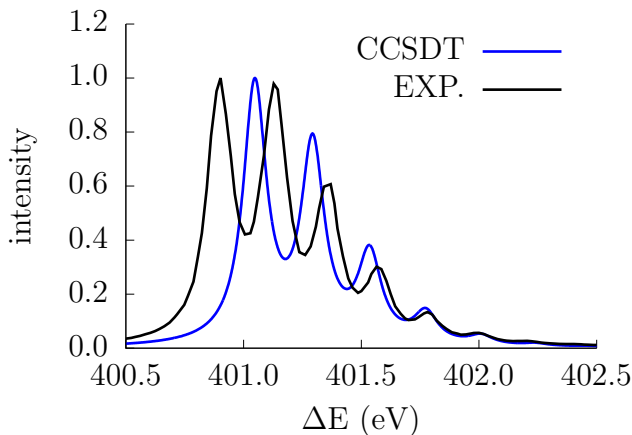


FIG. 5: Comparison of the first experimental peak with CCSDT using SFX2C-1e and the d-aug-cc-pCVQZ basis set.

and the vibrational separation is 0.03 eV too low. The corresponding errors for CCSD are 0.91 and 0.03 eV, both too high. Further enlarging the basis set will likely reduce the first excitation energy by several hundredth of eV since the CC3/aug-cc-pCV5Z result is 0.04 eV lower than the CC3/aug-cc-pCVQZ result. The excitation energy was also calculated using the asymmetric Lanczos algorithm with and without CVS in the aug-cc-pCVTZ basis. The excitation energy obtained from the solution of the full equation is 0.02 eV higher than the CVS result and the intensity is reduced by 6% when using CVS.

The intensities in the CC3 spectrum fall off too quickly compared to the experiment. We mention that the simulated vibrational structure is insensitive to the oscillator strength curve used in the calculation, and depends almost entirely on the quality of the PES. The

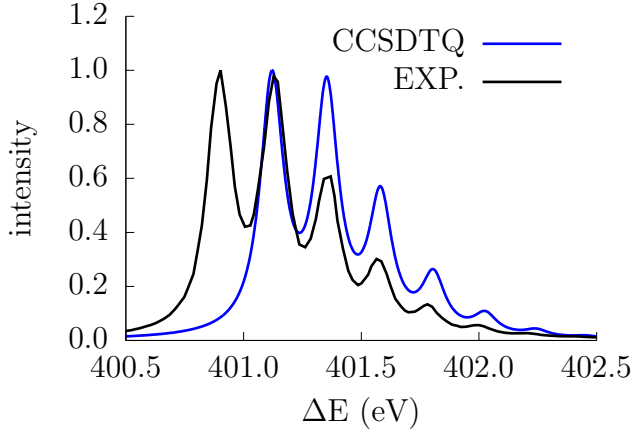


FIG. 6: Comparison of the first experimental peak with CCSDTQ using SFX2C-1e and the cc-pCVTZ basis.

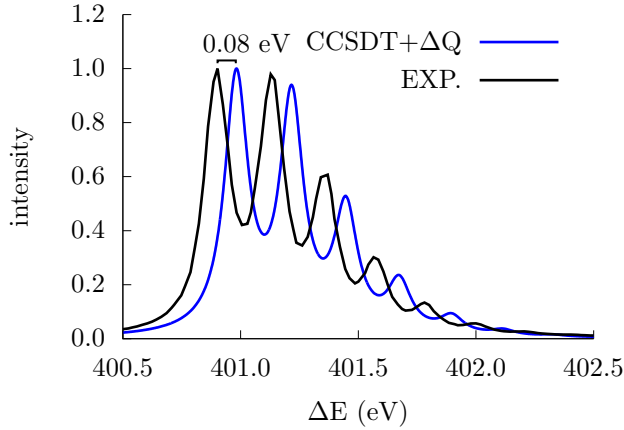


FIG. 7: Comparison of the first experimental peak with CCSDT using d-aug-cc-pCVQZ and SFX2C-1e and the quadruples contribution using cc-pCVTZ.

TABLE I: Positions in eV and intensities of the vibrational structure of the first excited state. **Energies for the higher vibrational transitions are given as the difference in vibrational energy from the previous state.** (Basis set: d-aug-cc-pCVQZ.)

transition	ADC(2)-x		CCSD		CC3		Experiment	
	ΔE	f	ΔE	f	ΔE	f	ΔE	f
$0 \rightarrow 0$	399.24	1.00	401.80	1.00	401.03	1.00	400.90	1.00
$0 \rightarrow 1$	+0.20	1.14	+0.27	0.52	+0.25	0.65	+0.23	0.95
$0 \rightarrow 2$	+0.20	0.76	+0.26	0.16	+0.25	0.25	+0.23	0.56
$0 \rightarrow 3$	+0.19	0.40	+0.26	0.04	+0.24	0.08	+0.22	0.24
$0 \rightarrow 4$	+0.18	0.18	+0.25	0.01	+0.24	0.02	+0.21	0.09
$0 \rightarrow 5$	+0.18	0.08	+0.25	0.00	+0.23	0.01	+0.21	0.04
$0 \rightarrow 6$	+0.17	0.03	+0.25	0.00	+0.23	0.00	+0.22	0.02

TABLE II: Positions in eV and intensities of the vibrational structure of the first excited state obtained using relativistic CCSDT/d-aug-cc-pCVQZ and CCSDTQ/cc-pCVTZ potential energy surfaces (SFX2C-1e model). The last two columns contain the CCSDT results with the quadruples from the smaller basis set added. **Energies for the higher vibrational transitions are given as the difference in vibrational energy from the previous state.**

transition	CCSDT		CCSDTQ		CCSDT+ Δ Q	
	ΔE	f	ΔE	f	ΔE	f
0 \rightarrow 0	401.05	1.00	401.12	1.00	400.98	1.00
0 \rightarrow 1	+0.25	0.76	+0.23	0.94	+0.23	0.91
0 \rightarrow 2	+0.24	0.34	+0.23	0.52	+0.23	0.48
0 \rightarrow 3	+0.24	0.12	+0.22	0.22	+0.23	0.19
0 \rightarrow 4	+0.24	0.03	+0.22	0.08	+0.22	0.07
0 \rightarrow 5	+0.23	0.01	+0.22	0.03	+0.22	0.02
0 \rightarrow 6	+0.23	0.00	+0.21	0.01	+0.21	0.01

vibrational analysis performed using a constant oscillator strength for all the geometries produces results almost identical to those obtained using CCSD oscillator strength curve. We thus decided to use the CCSD oscillator strength in all the CC simulations presented here. Comparing ADC(2)-x and CCSD in Table I, the ADC(2)-x potential is much shallower than the CC potentials, resulting in the vibrational levels being closer together. The CCSD potential is deeper than the CC3 potential, resulting in larger energy gaps.

In Figures 5, 6, and 7, the predicted peaks from CCSDT, CCSDTQ, and CCSDT+ Δ Q are compared to experiment and the numerical results are presented in Table II. All the results presented here have included scalar-relativistic effects via the SFX2C-1e scheme. The comparison of the SFX2C-1e and non-relativistic calculations shows that the scalar-relativistic effects increases the excitation energy by 0.21 eV throughout the PES. When taking the relativistic effects into account, the CCSDT and CCSDT+ Δ Q models lower the excitation energies by 0.19 and 0.26 eV in comparison to CC3. The excitation energies obtained using the CCSDT and CCSDT+ Δ Q models are 0.15 and 0.08 eV higher than the experimental value, respectively. The treatment of electron correlation in the CCSDTQ method is thus essentially quantitative for this property, considering that the remaining basis set effects will reduce the excitation energy by several hundredth of eV. The description of the intensities for the vibrational transitions are systematically improved along the CCSD, CCSDT, and CCSDT+ Δ Q series, with the CCSDT+ Δ Q model faithfully reproducing the

vibrational progressions in the experimental spectra. Interestingly, the CCSDTQ/cc-pCVTZ model produces the relative vibrational intensities even slightly better than the CCSDT+ Δ Q model, although the CCSDTQ/cc-pCVTZ excitation energy exhibits a larger error due to the use of a smaller basis set. This again indicates that the shape of the potential energy surface plays the most important role in the calculation of the relative intensities of the vibrational transitions. The minimum energy bond length of the core-excited state is significantly stretched compared to the ground state and the quadruple excitations are required for accurately describing this region **due to the high multireference character of nitrogen at stretched geometries**⁵⁰. For other molecules, CC3 and CCSDT may produce more accurate vibrational intensities.

The equilibrium bond length of the first core-excited potential is calculated to be 1.158 Å using both CC3 and CCSDT, while the CCSDTQ and CCSDT+ Δ Q values are both 1.172 Å. CC3 calculations using different basis sets have shown that the bond length for this state is insensitive to the choice of basis set. The experimental value is reported as 1.164 Å⁴⁷ which is closer to CC3 than to CCSDTQ. Note that this so-called “experimental equilibrium bond length” for the core-excited state was obtained as a parameter in a Morse potential that was fit to reproduce the experimental spectrum. Since the overall shape of the calculated PES substantially deviates from a Morse potential, a direct comparison between the computational and “experimental” values of the equilibrium bond length is not possible. We mention that the ADC(2)-x bond length is 1.187 Å and is substantially longer.

Positions and relative intensities of the Rydberg states are presented in Table III and the simulated CC3 spectrum is compared to the experimental spectrum in Figure 2. The energy gap between the first core-excited state and the first Rydberg state is calculated to be 5.20 eV with CC3, 0.06 eV lower than the experimental value. For comparison, the gap is 5.68 eV with ADC(2)-x and 5.57 eV with CCSD. For the gap between the two states, the error is less than 0.01 eV. We note that using the smaller basis set aug-cc-pCVQZ increased the gap from the first core-excited state by about 0.4 eV for all models.

The energy gaps between the vibrational states are both about 0.03 eV too high for the Rydberg states, indicating that the calculated PES are too deep. Intensities are also too weak for both the $0 \rightarrow 0$ transitions, especially for the $^1\Pi_u$ state. The $0 \rightarrow 1$ transitions, on the other hand, are too strong. In this case it is possible that the error occurs due to the CCSD intensities being too low relative to the first excited state. Furthermore, the $0 \rightarrow 1$

TABLE III: Positions in eV and relative intensities of the vibrational structure of the Rydberg states. Higher vibrational transitions indicated relative to the previous transition. (Basis set: d-aug-cc-pCVQZ.)

transition	CC3		Experiment	
	ΔE	$f \times 10$	ΔE	$f \times 10$
$^1\Sigma_u^+ 0 \rightarrow 0$	406.23	0.29	406.16	0.36
$^1\Sigma_u^+ 0 \rightarrow 1$	+0.31	0.07	+0.29	0.03
$^1\Pi_u^+ 0 \rightarrow 0$	407.22	0.53	407.15	0.91
$^1\Sigma_u^+ 0 \rightarrow 0$	407.41	0.03	407.36	0.02
$^1\Pi_u^+ 0 \rightarrow 1$	+0.32	0.14	+0.28	0.13

transitions are quite weak and the peaks are convoluted with other states, so it is challenging to obtain accurate intensities, especially for the weak $^1\Sigma_u^+$ state.

In Figure 8 we have plotted the CC3 PES of the states. We have also indicated the relevant vibrational levels with horizontal lines. For the first core-excited state, the equilibrium bond length is stretched compared to the ground state, while those for the Rydberg states are slightly compressed. When the bond is stretched, the higher $^1\Sigma_u^+$ state goes through a symmetry allowed intersection with the $^1\Pi_u$ state and an avoided crossing with the other $^1\Sigma_u^+$ state. Also, a large number of dark states whose transitions are forbidden by symmetry are not shown in the figure.

In Figure 9 the change in the electron density between the ground state and the first $^1\Pi_u$ state is plotted using Molden⁵¹. The density is plotted in a plane containing the N_2 molecule and in 3D using isosurfaces. A large density reduction is observed in the cores and a corresponding increase occurs with π symmetry. We note that a superposition of the two core holes is formed because the two atoms are equivalent, **consistent with experiments**⁵².

IV. CONCLUSION

Calculating core-excited states is challenging, not just because of the difficulties of finding the corresponding eigenvalues, but also because of the large relaxation effects that occur. For the lowest energy core-excited state of nitrogen, the deviation of CCSD from CC3 is almost 0.8 eV, considerably higher than the typical deviation of 0.2 eV for valence-excited states⁵³. In addition, large basis sets are required with extra functions to describe the core electrons. For the excited states with Rydberg nature, doubly augmented basis sets are

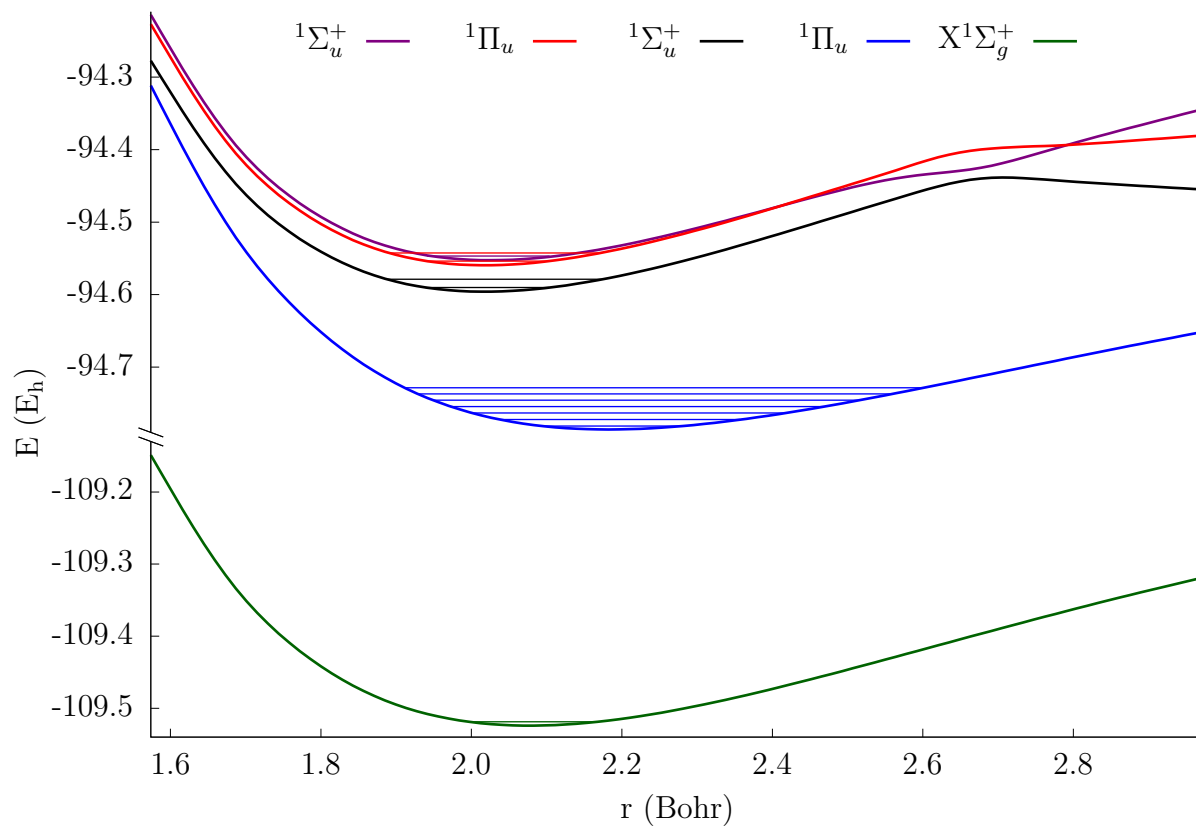


FIG. 8: Potential energy surfaces of ground and excited states and vibrational levels calculated with CC3/d-aug-cc-pCVQZ.



FIG. 9: Difference in electron density between the ground state and the lowest energy ${}^1\Pi_u$ core-excited state in the plane and as isosurfaces. Red indicates reduced density and blue increased. Isovalue: 0.01

necessary to get the correct energies. Nevertheless, we have demonstrated that CC3 can predict spectra with sufficient accuracy to assign peaks to states. In order to reproduce the vibrational spectra, a highly accurate PES is required. CCSDT improves both the shape of the PES and the absolute excitation energy, while CCSDTQ is required to accurately reproduce the vibrational spectrum quantitatively. **We note that nitrogen is a somewhat special case with strongly interacting core holes, which complicates the description of the core relaxation.** CC3 may nonetheless be more accurate when describing excitations from single core orbitals.

We note that basis set requirements can be relaxed by utilizing the fact that the excitation is very local and the large basis set is only needed on the atom being excited. Furthermore, multilevel CC3 can reduce the computational cost by two orders of magnitude³⁰.

Vibrational effects can be important in NEXAFS spectra and are required when calculating the spectrum of N₂ to describe the vibrational structure and shifts in peak positions due to the zero point energy. Furthermore, scalar-relativistic effects are not negligible for accurate calculations of core excitation energies, even for a molecule that contains only a first-row element. Scalar-relativistic contributions obtained using the SFX2C-1e scheme increase the core-excitation energy of nitrogen by 0.21 eV throughout the PES.

ACKNOWLEDGMENTS

We thank T. J. Martinez for hosting part of this project at Stanford University and acknowledge computer time from NOTUR through project nn2962k. H.K. acknowledges financial support from the FP7-PEOPLE-2013-IOF funding scheme (Project No. 625321) and the Norwegian Research Council through FRINATEK project no. 263110/F20. R.H.M. acknowledges financial support from the COST action “XUV/X-ray light and fast ions for ultrafast chemistry (XLIC)”, ERC-STG-2014 under grant No 639508 and from the Research Council of Norway through its Centres of Excellence scheme, project number 262695. S.C. acknowledges financial support from the AIAS-COFUND program (Grant agreement No. 609033) **and from DTU Chemistry**. L.C. is grateful to Johns Hopkins University for the start-up fund and the computing time at Maryland advanced research computing center (MARCC). M.G. acknowledges funding via a Lichtenberg Professorship from the Volkswagen Foundation. T.J.A.W. thanks the German National Academy of Sciences Leopoldina for

a fellowship (Grant No. LPDS2013-14). Parts of this research were carried out at the PLEIADES beamline, Soleil Synchrotron, France, proposal number 20141088.

REFERENCES

- ¹F. Holch, D. Hübner, R. Fink, A. Schöll, and E. Umbach, *J. Electron Spectrosc. Relat. Phenom.* **184**, 452 (2011).
- ²C. Garino, E. Borfecchia, R. Gobetto, J. A. van Bokhoven, and C. Lamberti, *Coordin. Chem. Rev.* **277**, 130 (2014), following Chemical Structures using Synchrotron Radiation.
- ³J. Stöhr, *NEXAFS Spectroscopy*, 1st ed. (Springer-Verlag Berlin Heidelberg, New York, 1992).
- ⁴M. Chergui and E. Collet, *Chem. Rev.* **117**, 11025 (2017), PMID: 28692268, <http://dx.doi.org/10.1021/acs.chemrev.6b00831>.
- ⁵O. Plekan, V. Feyer, R. Richter, M. Coreno, M. de Simone, K. Prince, A. Trofimov, E. Gromov, I. Zaytseva, and J. Schirmer, *Chem. Phys.* **347**, 360 (2008).
- ⁶V. Feyer, O. Plekan, R. Richter, M. Coreno, M. de Simone, K. C. Prince, A. B. Trofimov, I. L. Zaytseva, and J. Schirmer, *J. Phys. Chem. A* **114**, 10270 (2010).
- ⁷T. J. A. Wolf, R. H. Myhre, J. P. Cryan, A. Battistoni, N. Berrah, C. Bostedt, P. Bucksbaum, R. N. Coffee, G. Coslovich, R. Feifel, K. J. Gaffney, J. Grilj, T. J. Martínez, S. Miyabe, S. P. Moeller, M. Mucke, A. Natan, R. Obaid, T. Osipov, O. Plekan, S. Wang, H. Koch, and M. Gühr, *Nat. Comm.* **8**, 2041 (2017), <https://doi.org/10.1038/s41467-017-00069-7>.
- ⁸A. R. Attar, A. Bhattacharjee, C. D. Pemmaraju, K. Schnorr, K. D. Closser, D. Prendergast, and S. R. Leone, *Science* **356**, 54 (2017), <http://science.sciencemag.org/content/356/6333/54.full.pdf>.
- ⁹T. Popmintchev, M.-C. Chen, D. Popmintchev, P. Arpin, S. Brown, S. Ališauskas, G. Andriukaitis, T. Balčiūnas, O. D. Mücke, A. Pugzlys, A. Baltuška, B. Shim, S. E. Schrauth, A. Gaeta, C. Hernández-García, L. Plaja, A. Becker, A. Jaron-Becker, M. M. Murnane, and H. C. Kapteyn, *Science* **336**, 1287 (2012), <http://science.sciencemag.org/content/336/6086/1287.full.pdf>.
- ¹⁰A. Picón, C. S. Lehmann, C. B. A. Rudenko, A. Marinelli, T. Osipov, D. Rolles, N. Berrah, C. Bomme, M. Bucher, G. Doumy, B. Erk, K. R. Ferguson, T. Gorkhover, P. J. Ho,

- E. P. Kanter, B. Krässig, J. Krzywinski, A. A. Lutman, A. M. March, D. Moonshiram, D. Ray, L. Young, S. T. Pratt, and S. H. Southworth, *Nat. Comm.* **7**, 11652 (2016), <http://dx.doi.org/10.1038/ncomms11652>.
- ¹¹S. M. Teichmann, F. Silva, S. L. Cousin, M. Hemmer, and J. Biegert, *Nat. Comm.* **7**, 11493 (2016), <http://dx.doi.org/10.1038/ncomms11493>.
- ¹²Y. Pertot, C. Schmidt, M. Matthews, A. Chauvet, M. Huppert, V. Svoboda, A. von Conta, A. Tehlar, D. Baykusheva, J.-P. Wolf, and H. J. Wörner, *Science* **355**, 264 (2017), <http://science.sciencemag.org/content/355/6322/264.full.pdf>.
- ¹³J. Wenzel, M. Wormit, and A. Dreuw, *J. Comput. Chem.* **35**, 1900 (2014).
- ¹⁴S. Fatehi, C. P. Schwartz, R. J. Saykally, and D. Prendergast, *J. Chem. Phys.* **132**, 094302 (2010), <http://dx.doi.org/10.1063/1.3324889>.
- ¹⁵O. Plekan, V. Feyer, R. Richter, M. Coreno, M. de Simone, K. Prince, and V. Carravetta, *J. Electron Spectrosc. Relat. Phenom.* **155**, 47 (2007).
- ¹⁶I. Bâldea, B. Schimmelpfennig, M. Plaschke, J. Rothe, J. Schirmer, A. Trofimov, and T. Fanghnel, *J. Electron Spectrosc. Relat. Phenom.* **154**, 109 (2007).
- ¹⁷S. Coriani, T. Fransson, O. Christiansen, and P. Norman, *J Chem. Theory Comput.* **8**, 1616 (2012), <http://dx.doi.org/10.1021/ct200919e>.
- ¹⁸J. Wenzel, M. Wormit, and A. Dreuw, *J. Chem. Theory Comput.* **10**, 4583 (2014).
- ¹⁹E. J. Davidson, *J. Comp. Phys.* **17**, 87 (1975).
- ²⁰P. S. Bagus, *Phys. Rev.* **139**, A619 (1965).
- ²¹C. Lanczos, *J. Res. Nat. Bur. Stand.* **45**, 225 (1950).
- ²²S. Coriani, O. Christiansen, T. Fransson, and P. Norman, *Phys. Rev. A* **85**, 022507 (2012).
- ²³S. H. Southworth, R. Wehlitz, A. Picón, C. S. Lehmann, L. Cheng, and J. F. Stanton, *J. Chem. Phys.* **142**, 224302 (2015), <http://dx.doi.org/10.1063/1.4922208>.
- ²⁴L. S. Cederbaum, W. Domcke, and J. Schirmer, *Phys. Rev. A* **22**, 206 (1980).
- ²⁵A. Barth and J. Schirmer, *J. Phys. B: At. Mol. Phys.* **18**, 867 (1985).
- ²⁶A. B. Trofimov, T. É. Moskovskaya, E. V. Gromov, N. M. Vitkovskaya, and J. Schirmer, *J. Struct. Chem.* **41**, 483 (2000).
- ²⁷M. Wormit, D. R. Rehn, P. H. Harbach, J. Wenzel, C. M. Krauter, E. Epifanovsky, and A. Dreuw, *Mol. Phys.* **112**, 774 (2014), <http://dx.doi.org/10.1080/00268976.2013.859313>.
- ²⁸S. Coriani and H. Koch, *J. Chem. Phys.* **143**, 181103 (2015).
- ²⁹H. Koch, O. Christiansen, P. Jørgensen, A. M. Sánchez de Merás, and T. Helgaker, J.

- Chem. Phys. **106**, 1808 (1997).
- ³⁰R. H. Myhre and H. Koch, J. Chem. Phys. **145**, 044111 (2016), <http://dx.doi.org/10.1063/1.4959373>.
- ³¹D. A. Matthews and J. F. Stanton, J. Chem. Phys. **142**, 064108 (2015), <http://dx.doi.org/10.1063/1.4907278>.
- ³²J. H. Baraban, D. A. Matthews, and J. F. Stanton, J. Chem. Phys. **144**, 111102 (2016), <http://dx.doi.org/10.1063/1.4943865>.
- ³³K. G. Dyall, J. Chem. Phys. **106**, 9618 (1997), <http://dx.doi.org/10.1063/1.473860>.
- ³⁴W. Liu and D. Peng, J. Chem. Phys. **131**, 031104 (2009), <http://dx.doi.org/10.1063/1.3159445>.
- ³⁵H. Koch and P. Jørgensen, J. Chem. Phys. **93**, 3333 (1990).
- ³⁶T. B. Pedersen and H. Koch, J. Chem. Phys. **106**, 8059 (1997).
- ³⁷J. F. Stanton and R. J. Bartlett, J. Chem. Phys. **98**, 7029 (1993).
- ³⁸K. Aidas *et al.*, WIREs Comput. Mol. Sci. **4**, 269 (2014).
- ³⁹J. F. Stanton *et al.*, “CFOUR, coupled-cluster techniques for computational chemistry <http://www.cfour.de>,” (2015).
- ⁴⁰L. Cheng and J. Gauss, J. Chem. Phys. **135**, 084114 (2011), <http://dx.doi.org/10.1063/1.3624397>.
- ⁴¹Y. Shao *et al.*, Mol. Phys. **113**, 184 (2015), <http://dx.doi.org/10.1080/00268976.2014.952696>.
- ⁴²D. Sundholm, J. Gauss, and A. Schäfer, J. Chem. Phys. **105**, 11051 (1996).
- ⁴³D. E. Woon and T. H. Dunning, J. Chem. Phys. **103**, 4572 (1995).
- ⁴⁴R. A. Kendall, T. H. Dunning, and R. J. Harrison, J. Chem. Phys. **96**, 6796 (1992).
- ⁴⁵R. H. Myhre, T. J. A. Wolf, L. Cheng, S. Nandi, S. Coriani, M. Gühr, and H. Koch, “A theoretical and experimental benchmark study of core-excited states in nitrogen, supplementary material,” (2018), Supplementary Material Document No.
- ⁴⁶C. Miron, C. Nicolas, O. Travnikova, P. Morin, Y. Sun, F. Gel'mukhanov, N. Kosugi, and V. Kimberg, Nat. Phys. **8**, 1745 (2012).
- ⁴⁷C. T. Chen, Y. Ma, and F. Sette, Phys. Rev. A **40**, 6737 (1989).
- ⁴⁸R. N. Sodhi and C. Brion, J. Electron Spectrosc. Relat. Phenom. **34**, 363 (1984).
- ⁴⁹<https://www.synchrotron-soleil.fr/en/beamlines/pleiades>.
- ⁵⁰D. I. Lyakh, M. Musiał, V. F. Lotrich, and R. J. Bartlett, Chem. Rev. **112**, 182 (2012), <http://dx.doi.org/10.1021/cr2001417>.

- ⁵¹G.Schaftenaar and J. Noordik, *J. Comput.-Aided Mol. Design* **14**, 123 (2000).
- ⁵²M. S. Schöffler, J. Titze, N. Petridis, T. Jahnke, K. Cole, L. P. H. Schmidt, A. Cza-
sch, D. Akoury, O. Jagutzki, J. B. Williams, N. A. Cherepkov, S. K. Semenov, C. W.
McCurdy, T. N. Rescigno, C. L. Cocke, T. Osipov, S. Lee, M. H. Prior, A. Belkacem,
A. L. Landers, H. Schmidt-Böcking, T. Weber, and R. Dörner, *Science* **320**, 920 (2008),
<http://science.sciencemag.org/content/320/5878/920.full.pdf>.
- ⁵³D. Kánnár and P. G. Szalay, *J. Chem. Theory Comput.* **10**, 3757 (2014).